Journal of Electroceramics, 15, 83–93, 2005

Investigation of the Partial Oxidation of Methane at the Interface Metal (Pt, Au)|YSZ

S. ŻUREK,[1] M. MOSIAŁEK,[1] P. TOMCZYK[1,*]& D. OBŁĄKOWSKA[2]

[1]*Institute of Physical Chemistry of the Polish Academy of Sciences, Department of Molten Salts, ul. Zagrody 13, 30-318 Krakow, Poland*
[2]*AGH-University of Science and Technology, Faculty of Fuels and Energy, al. Mickiewicza 30, 30-059 Krakow, Poland*

Abstract. The reactions occurring at the electrodes of Pt|YSZ|Au cell fed with a mixture of CH_4+air were investigated at 600–850°C. The electrodes of this cell were made from Pt and Au wires, providing a small contact area between metal and YSZ (quasi-point electrodes). The dependences of the cell voltage on the composition of gas mixture and time were studied. A sequence of chemical and electrochemical reactions was proposed to explain the observed abrupt variation of the cell voltage from positive to negative values. Also the impedances of the Pt and Au electrodes were measured and analysed in order to justify the proposed mechanism of reactions.

Keywords: one-chamber fuel cell, methane oxidation, YSZ, impedance spectroscopy

1. Introduction

This work has been inspired by the development of a one-chamber fuel cell, which recently has accomplished pronounced achievements in increasing power density and utilization of carbonaceous fuel [1–5]. A conventional fuel cell is fed separately by fuel and oxidant supplied to two gas compartments, anodic and cathodic. Hence, different electrode reactions occur at the anode and cathode even if the electrodes are made of the same material. The one-chamber fuel cell is fed by a mixture of fuel and oxidant, which is simultaneously delivered to both electrodes. These electrodes are made of different materials, therefore they have different electrocatalytic activities that promote the oxidation of fuel at the anode and reduction of oxidant at the cathode. In this way the cell generates voltage and in consequence electric power.

The Pt|YSZ|Au cell fed with a mixture of methane and air is a classical example of one-chamber fuel cell [2–4]. The higher catalytic activity of Pt than Au for the partial oxidation reaction of methane is well recognized whereas Au is believed to be not much worse catalyst for the oxygen reduction than Pt. The best performance of the one-chamber fuel cell fed with CH_4+air has been reached for the Ni|YSZ|LSM and (GDC)Ni|YSZ|LSM (MnO_2) cells [4].

Our works are generally aimed at the investigation of processes occurring in the one-chamber fuel cell. However, on the contrary to the porous electrodes in the state-of-the-art fuel cell, we use micro-electrodes made of solid metal, called hereafter as quasi-point electrodes. At such electrodes, the processes are less complicated and therefore the mechanism of reaction can more easily be identified. In this work, we present the studies for the Pt|YSZ|Au cell. Investigations with a cell that employs composite electrodes are now under way.

2. Experimental

The cross section of the cell is shown in Fig. 1. The YSZ disk (8 mol.% yttria, 10 mm diameter and ca. 3 mm thick) was sintered at 1570°C from powder of the following characteristics: surface area $\sim$10 m^2g^{-1}, average particle size $<$0.5 μm, sinterability $\sim$98% of theoretical at T_s $<$ 1300°C and purity $>$99.95%, produced at Department of Ceramics and Materials

*To whom all correspondence should be addressed. E-mail: ptomczyk@uci.agh.edu.pl

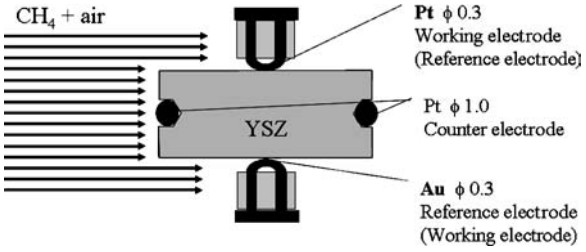

Fig. 1. Cross section of the measurement cell. The counter electrode is only seen at the edges of electrolyte.

Science of AGH-University of Science and Technology in Krakow. A 1 mm wide and 1 mm deep furrow was grooved around the side surface of the disk just in the middle of the side; the furrow was smeared with platinum paste before fixing a platinum wire (1 mm in diameter). This platinum wire was used as a counter electrode in the electrochemical measurements performed.

Both flat sides of the disk were polished with a 3000 waterproof alumina abrasive paper and afterwards 1 μm diamond paste. Two quasi-point electrodes were placed at the polished surfaces, one opposite the other as is shown in Fig. 1. The quasi-point electrode was made by passing a 0.3 mm wire throughout two holes of alumina bead—one electrode was made from gold wire and the other from platinum wire. The electrodes and disk were assembled inside an alumina holder and gripped together due to action of springs with a force of about 0.5 N. The cell with the holder were then placed inside an alumina envelope, which provided a gas-tight separation from the outer atmosphere. Finally, the whole system was put into a horizontal electric furnace.

An inlet of the gases was located a few millimetres from the side wall of the disk providing the gases to flow directly to the electrodes. A set up of gas flow controllers allowed to control the composition and flow rates of gases introduced into the cell.

Before the experiment, the cell was heated to 950–1000°C and held about one hour at this temperature. In these conditions, gold and platinum became soft and the quasi-point electrodes, pressed by the springs to the disk, increased contact areas between metal and YSZ. These contact areas could be determined after completing the experiment, when the cell was disassembled and the electrodes were examined with a metallurgical microscope. The flattened part of metal surface corresponded to the area that was in direct contact with the YSZ. The contact area of the Au electrode was 0.5–0.8 mm^2, whereas the surface of the Pt electrode was almost unaffected and the contact area of this electrode was estimated at about 0.02–0.03 mm^2.

After heating the cell to 950–1000°C for about one hour, the temperature was decreased to 750°C and the cell was left about 24 h under the flow of air. The cell was still kept under air, when the next day the temperature was risen/decreased to the desired measurement temperature. To provide similar initial conditions and minimize long-lasting memory effects of YSZ electrolyte [6–8], the cell was always kept about 24 h under air at 750°C before each experimental series.

After one hour since the stabilization of the measurement temperature, the mixture of CH_4+air was introduced to the cell. The response of the cell was almost immediate—its voltage, ΔE, became distinctly different from 0.000 V observed under air. The ratio of the partial pressures of methane and oxygen, for the first mixture introduced to the cell, was equal to $p(CH_4)/p(O_2) = 0.25$. The concentration of CH_4 in air was then increased every hour by a constant factor, so that the composition of consecutive mixtures corresponded to $p(CH_4)/p(O_2) = 0.25$, 0.375, 0.5, 0.625, 0.75... This procedure was continued until the voltage of the cell decreased to the considerably negative values (ΔE<–0.35 V). Then we held the conditions of the measurements stable for one hour. Afterwards the pure air was again supplied to the electrodes. The response of the cell appeared to be almost independent of the total flow rate of the gaseous mixture within the wide range extending from 5 to 1000 cm^3/minute. This indicated that the concentration of methane in the vicinity of electrodes was the same as in the input mixture within this range of flow rates. The flow rate was kept during the measurements at the level of 15–20 cm^3/minute.

The impedance measurements of the quasi-point electrodes were carried out simultaneously with the investigation of the cell voltage. When the impedance of the Pt quasi-point electrode was measured, the Au quasi-point electrode served as a reference electrode and vice versa. The impedance of the counter electrode could be neglected because of much larger contact area with the YSZ in comparison to the quasi-point electrodes.

The electrochemical measurements were performed with an IM5d Impedance Spectrum Analyser, a product

of Zahner Elektrik, Kronach. The dependences of the cell voltage on time were recorded using PVI software, provided by the producer. This option enables also recording impedance characteristics at an arbitrarily chosen moment. Generally, the frequency range used in the impedance measurements was 0.1 to 500,000 Hz. The amplitude of the sinusoidal voltage signal was 10 mV. For analysis of the impedance data, a program based on a complex non-linear regression least-squares (CNRLS) fit was used. This program was also provided by the producer.

3. Results

3.1. Voltage of the Cell

Typical curves that illustrate the cell voltages as a function of CH_4 concentration in air and time at temperatures 750, 800 and 850°C are shown in Fig. 2.

The following can be seen from these dependences:

(a) initially, at low concentrations of methane in air, the voltage of the cell was always positive and increased stepwise after each consecutive rise of CH_4 concentration. This effect was contrary to the expected variation of the cell voltage to negative values. Therefore, cells with two Pt and two Au electrodes were also tested to check if we were merely observing an artifact. When the electrodes were made of the same material, the cell voltage was always zero regardless of atmosphere;
(b) afterwards, there was a relative stabilization of the cell voltage; this lasted for a longer amount of time at lower temperatures;
(c) at last, an abrupt variation of the cell voltage to negative values occurred—frequently, in two consecutive steps;
(d) at the lower temperatures the abrupt variation of the cell voltage occurred at higher content of CH_4 in air.

The dependences of the cell voltage on the time that elapsed since introducing the CH_4+air mixture were also determined. These studies were performed in the temperature range from 600 to 825°C. The concentration of CH_4+air mixture was kept constant and corresponded to $p(CH_4)/p(O_2) = 1$. At temperatures below 700°C, no abrupt variation of the cell voltage to negative values was observed within duration of 50 h. The dependences recorded at the temperatures higher than 700°C are shown in Fig. 3.

At 800 and 825°C, the cell voltage was positive within a few initial minutes of the experiment (up to ΔE = ca. +0.1 V), then the steep decrease of the voltage was observed (down to ΔE = ca. −0.6 V). Afterwards, the voltage of the cell increased gradually up to $\Delta E = -(0.05–0.1)$ V in duration of 40–50 h. At

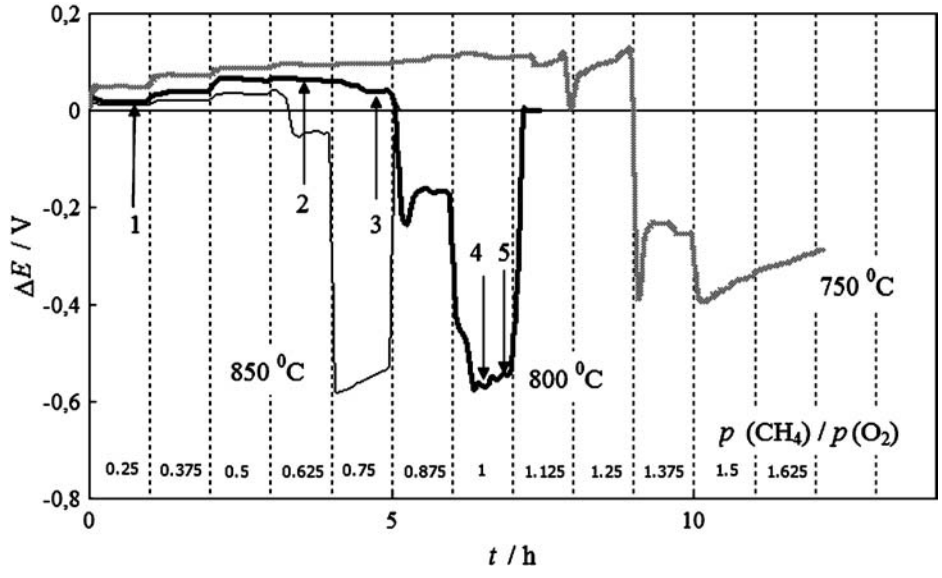

Fig. 2. Dependences of the cell voltage on the time and composition of CH_4+air mixture. The dependences were recorded at 750, 800 and 850°C. The impedances spectra were recorded at the times indicates by arrows.

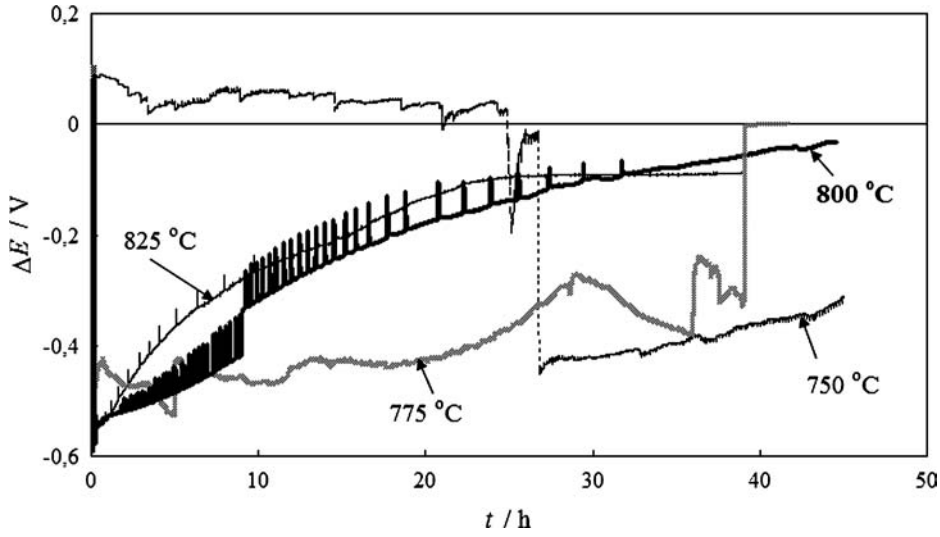

Fig. 3. Time dependences of the cell voltage at various temperatures [$p(CH_4)/p(O_2) = 1$].

775°C, this increase was not as rapid as at the higher temperatures and proceeded in an irregular way. At 750°C, the abrupt variation of the cell voltage occurred after ca. 25 h since introducing the CH_4+air mixture to the vessel. There is a clear coincidence between the temperature and behaviour of the voltage-time curves: as the temperature is increased, the abrupt variation of the cell voltage appears sooner. The irregular jumps and spikes at these dependences may indicate that an active solid state reagent deposits at the surface of the cell electrode. Indeed, the Pt working and auxiliary electrodes were covered with a layer of carbon (black or/and whisker) after prolonged operation of the cell in the range of negative voltages. Sometimes, the carbon deposit spread from the Pt electrodes to the whole surface of the cell. This resulted in a short circuit between electrodes.

3.2. Impedances of the Quasi-Point Electrodes

The impedance measurements were carried out at 800°C. The spectra were recorded at the times pointed out by arrows in Fig. 2. The complex plane plots of the impedance for both the quasi-point electrodes at the rest potential are shown in Figs. 4 and 5. As can be seen, the impedances of the Au electrode, determined after various times since introducing the CH_4+air mixture, do not differ much between themselves. The considerable deviation from the family of curves is observed only in the case of pure air atmosphere. This means that the concentration O_2 in the CH_4+air mixture at the Au electrode remains significant during the whole experimental series—the oxygen electrode reaction still prevails although influence of other processes is also evident. The most apparent effect of these additional reactions appears when the atmosphere of pure air is switched to CH_4+air. On the contrary to the Au electrode, the impedance of the Pt electrode changes considerably during the experiment. Pt is a good catalyst for the partial oxidation of methane and therefore, in the vicinity of Pt electrode, the composition of gases is close to that in the equilibrium conditions. The equilibrium concentrations depend strongly on the initial ratio of $p(CH_4)/p(O_2)$ in the gas mixture introduced to the cell. Because this ratio is varied during the experiment, the diversity in the response of the Pt electrode is observed.

To explain the behaviour of the Pt electrode more precisely, the further impedance investigations were focused on this electrode exclusively. The Nyquist plots for the quasi-point Pt electrode at various potentials are shown in Figs. 6–8. The data presented in Fig. 6 were recorded when the atmosphere of pure air was kept in the vessel. Figures 7 and 8 show the impedances of the Pt electrode before and after the abrupt variation of the cell voltage from the positive to negative values, respectively. During these measurements, the CH_4+air mixture had been introduced to the cell.

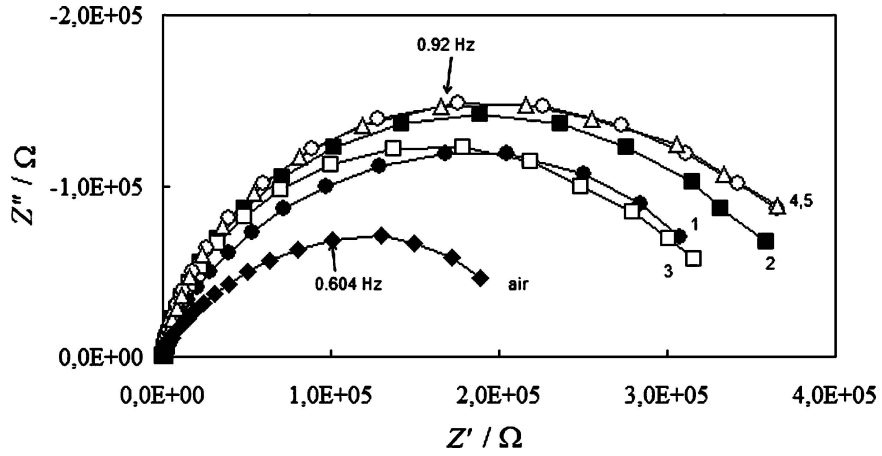

Fig. 4. Nyquist plots for the impedances of the Au quasi-point electrode at the rest potential in the air (♦) and CH_4+air mixtures at the moments indicated by numbers in Fig. 2: (●) 1, (■) 2, (□) 3, (○) 4 and (△) 5. Temperature: 800°C.

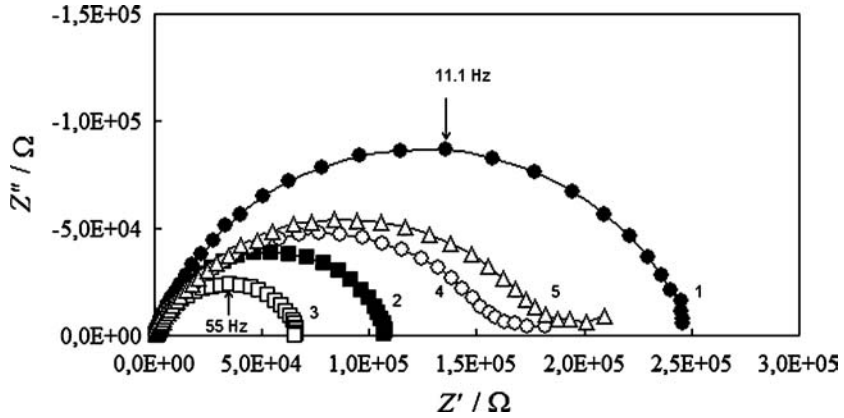

Fig. 5. Nyquist plots for the impedances of the Pt quasi-point electrode at the rest potential in the CH_4+air mixtures at the moments indicated by the numbers in Fig. 2. Notations as in Fig. 4.

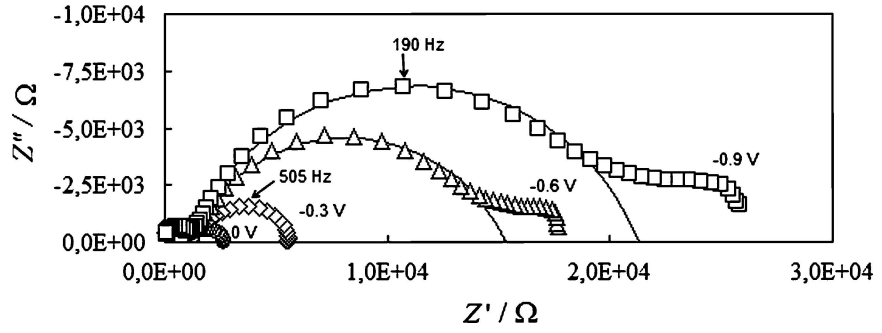

Fig. 6. Nyquist plots for the impedances of the Pt quasi-point electrode at 800°C at various voltages measured vs. the Au electrode: (○) 0.0 V, (∗) –0.3 V, (△) –0.6 V and (□) –0.9 V. Lines correspond to the CNRLS fit. Air over the electrode.

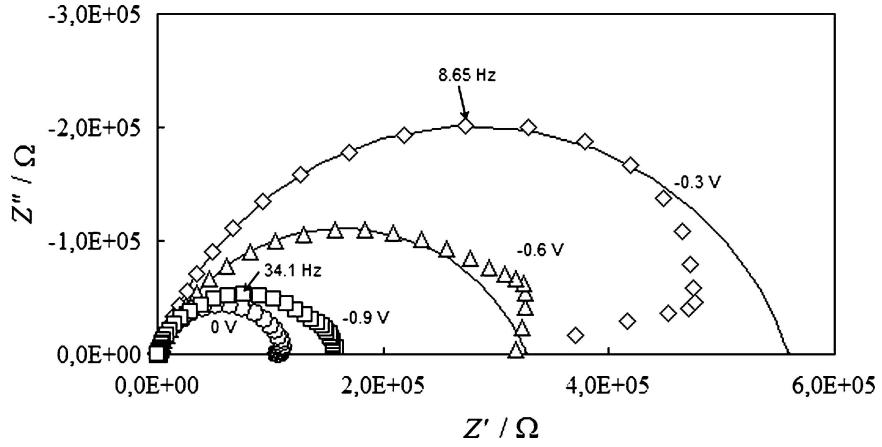

Fig. 7. Nyquist plots for the impedances of the Pt quasi-point electrode at 800°C at the various voltages measured vs. the Au electrode. Notations as in Fig. 6. CH_4+air [$p(CH_4)/p(O_2) = 0.75$] over the electrode. Before the abrupt variation of the cell voltage to the negative values.

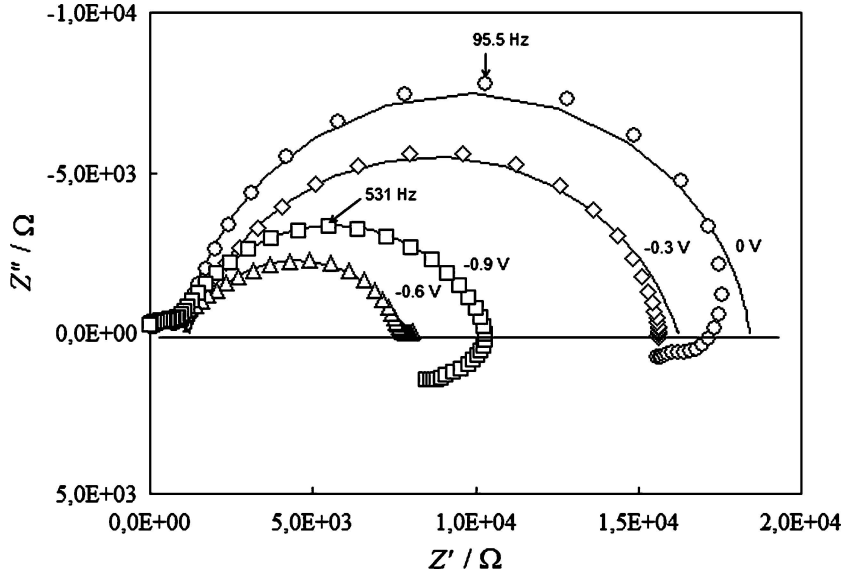

Fig. 8. Nyquist plots for the impedances of the Pt quasi-point electrode at 800°C at various voltages measured vs. the Au electrode. Notations as in Fig. 6. CH_4+air [$p(CH_4)/p(O_2) = 0.875$] over the electrode. After the abrupt variation of the cell voltage.

Generally, two arcs can be distinguished at the plots presented in Figs. 6–8. Usually, the arcs at high frequencies characterize the contact and electrolyte impedances whereas these at low frequencies are related to the electrode polarization impedances [9–11]. We assumed that in the limited range of low frequencies (below 20–1000 Hz), the latter arc can be modeled by the response of a simplified equivalent circuit $R_s(R_e Q)$, where R_s is the contact and ohmic resistance of the electrolyte, R_e is the electrode polarization resistance and Q is the constant phase element, whose impedance is defined as

$$Z_Q = 1/[Q(j\omega)^{\phi}] \tag{1}$$

ω is the angular rate, $j = (-1)^{1/2}$, Q is a constant and ϕ may vary between -1 (ideal inductance) and 1 (ideal capacitance). The values of R_s, R_e, Q and ϕ were determined by fitting the response of the equivalent circuit to the experimentally measured impedances with the CN-

RLS method. At very low frequencies, irregular deviations from the arc fitted with the CNRLS method are observed. Similar phenomenon, the so called, inductive loop, was observed for some electrode processes occurring at metal|YSZ electrolyte interface [6–8, 12–15]. It has been attributed to "crosstalk" between the working and reference electrodes [12], accumulation of intermediate species in multistep mechanisms [8], increase of the fraction of coverage of one of adsorbed species [15] or deposition of carbon [13].

For the Pt electrode kept under the atmospheres of pure air and CH_4+air mixture before the abrupt variation of the cell voltage, $R_s = 1.1 \pm 0.1$ kΩ and is almost independent of ΔE. According to the Newmann equation [16]:

$$R_{\mathrm{el}} = 1/(4r\sigma_{\mathrm{el}}) \tag{2}$$

where R_{el} is the electrolyte resistance determined by impedance spectroscopy, σ_{el} is the specific conductivity of the electrolyte and r is the effective contact radius. Taking $\sigma_{\mathrm{el}} = 0.02\ \Omega^{-1}\ \mathrm{cm}^{-1}$ equal to the ionic conductivity of 8–10% Y_2O_3 doped ZrO_2 at 800°C [17] and $r = 0.01$ cm equal to the radius of the circle that corresponds to the contact area of the Pt electrode (0.03 mm^2), we get $R_{\mathrm{el}} = 1.2$ kΩ. This value is very close to R_s determined from the EIS measurements and means that the contact resistance of Pt electrode is insignificant compared to the ohmic resistance of electrolyte. After the abrupt variation of the cell voltage to the negative values, $R_s = 0.6 \pm 0.3$ kΩ. The variation of the cell voltage affects the value of R_s, which should remain approximately constant. Although the relative decrease of R_s is significant (over 45%), the difference between these two values only slightly exceed the sum of estimation errors. On the other hand, the carbon deposit after the variation of the cell voltage may increase the contact area of the Pt electrode. Hence, according to the Newmann equation (2), the deposition of carbon may give an apparent effect of decreasing R_s.

Before the abrupt variation of the Pt electrode, Q varies between 27 and 68 nF $s^{\phi-1}$ and ϕ between 0.73 and 0.91. The double layer capacitance for the Pt/YSZ interface is up to 1300 μm cm^{-2} [18]. For the CPE element, the capacitance can be calculated according to the formula [19]:

$$C = R_e^{(1-\phi)/\phi}\ Q^{1/\phi} \tag{3}$$

Using Eq. (3), we can estimate the double layer capacitance from the EIS measurements as equal to 770–1150 μF cm^{-2}, which is a reasonable value. After the abrupt variation of the cell voltage, Q varies between 13 and 26 nF $s^{\phi-1}$and ϕ between 0.75 and 0.83.

The dependences of R_e on the potential difference between the Pt and Au electrodes are shown in Fig. 9.

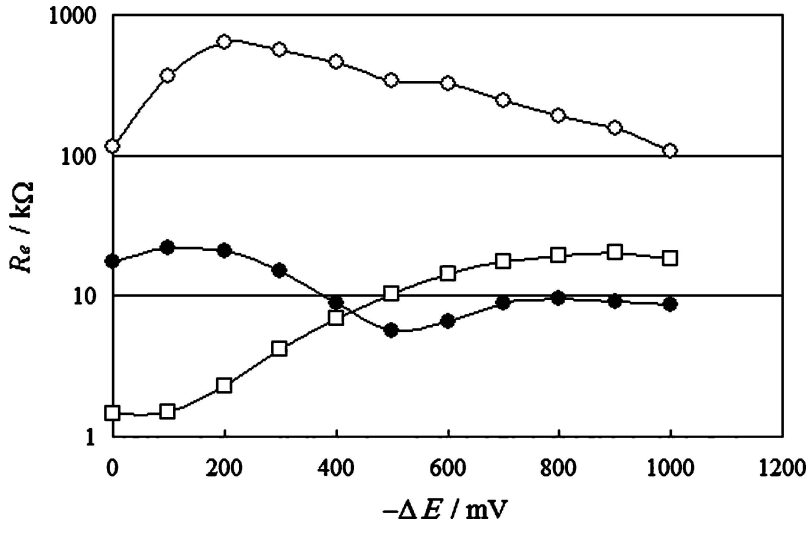

Fig. 9. Dependences of the electrode polarization resistance of the Pt quasi-point electrode on the voltage measured vs. the Au electrode. Conditions of the measurements: (□) air atmosphere, (○) $p(CH_4)/p(O_2) = 0.75$, before the abrupt variation of the cell voltage, (●) $p(CH_4)/p(O_2) = 0.875$, after the abrupt variation of the cell voltage. Temperature: 800°C.

As can be seen from the plots in Fig. 9:

1. The resistance R_e is the highest just a while before the abrupt variation of the cell voltage from positive to negative values. About one order of magnitude lower R_e values are observed after the abrupt variation of the cell voltage and when the pure air atmosphere is kept inside the cell. This behaviour indicates that concentrations of electroactive entities in the vicinity of the Pt electrode are considerably lower just before the variation of the cell voltage than after this variation or under the air atmosphere.
2. The minima of R_e appear at ca. 0 V when the Pt electrode is kept under air and ca. −0.5 V after the abrupt variation of the cell voltage. This reveals that the character of the electrode reactions at Pt changes: the reaction of oxygen electrode dominates in the atmosphere of pure air whereas the reaction with much lower standard potential prevails after the abrupt variation of the cell voltage, i.e. this reaction involves probably products of methane decomposition. The minimum at the dependences of R_e on the potential of the electrode appears when, for example, transport of electroactive entities affects electrode process—in the case of the semi-infinite linear diffusion, this minimum appears at $E_s = E_{1/2} + (RT/nF)\ln(\alpha/1-\alpha)$, where $E_{1/2}$ is the half-wave potential and α is the transfer coefficient [20].

4. Discussion

Partial oxidation (POX) is one of the principal processes for converting methane into synthesis gas. The POX reactions can be accelerated by a large number of different catalysts including noble metals: one of the most effective is Pt [21] whereas Au is considerably less active [22, 23].

The sequence of POX reactions [24], occurring when the content of methane in air increases, is given in Table 1 (non-electrodic reactions). These reactions are accompanied by the steam reforming and shift reactions. The products of non-electrodic reactions may participate at the Pt and Au electrodes in electrodic processes, whose equations are proposed in the last column of Table 1 (electrodic reaction). The phenomena described earlier in this work might be explained on the basis of these reaction mechanisms.

At the beginning of the experiment, for the initial concentration of CH_4 corresponding to $p(CH_4)/p(O_2) = 0.25$, the chemical reaction proceeding the electrode process is written in symbolic way in Table 1

Table 1. Sequence of dominant non-electrodic and electrodic reactions occurring at Pt and Au electrodes when content of methane in air increases.

No.	Electrode	$p(CH_4)/p(O_2)$	Non-electrodic reaction	Electrodic reaction
1.	Pt	0.125	$CH_4 + 8O_2 \overset{\leftarrow}{\rightarrow} CO_2 + 2H_2O + 6O_2$	$O_2 + 4e^- \overset{\leftarrow}{\rightarrow} 2O^{2-}$
2.		0.5	$CH_4 + 2O_2 \overset{\leftarrow}{\rightarrow} CO_2 + 2H_2O$	$\updownarrow$ Abrupt variation of cell voltage
3.		0.667	$CH_4 + 3/2O_2 \overset{\leftarrow}{\rightarrow} CO + 2H_2O$ $CO + H_2O \overset{\leftarrow}{\rightarrow} CO_2 + H_2$	$CO + O^{2-} \overset{\leftarrow}{\rightarrow} CO_2 + 2e^-$ $H_2 + O^{2-} \overset{\leftarrow}{\rightarrow} H_2O + 2e^-$
4.		1.0	$CH_4 + O_2 \overset{\leftarrow}{\rightarrow} CO + 2H_2O + H_2$ $CO + H_2O \overset{\leftarrow}{\rightarrow} CO_2 + H_2$	$CO + O^{2-} \overset{\leftarrow}{\rightarrow} CO_2 + 2e^-$ $H_2 + O^{2-}\ H_2O + 2e^-$
		>1.0	$CH_4 + H_2O \overset{\leftarrow}{\rightarrow} CO + 3H_2$	
5.		≥0.125	$CH_4 \overset{\leftarrow}{\rightarrow} C + 2H_2$	
		>0.5	$2CO \overset{\leftarrow}{\rightarrow} C + CO_2$	$C + O^{2-} \overset{\leftarrow}{\rightarrow} CO + 2e^-$
		>0.667	$CO + H_2 \overset{\leftarrow}{\rightarrow} C + H_2O$	
6.	Au	≥0		$O_2 + 4e^- \overset{\leftarrow}{\rightarrow} 2O^{2-}$ $\updownarrow$ Mixed potential
			Small effect of reaction	
7.		≥0.125	$CH_4 + O_2 \rightarrow CO_2 + 2H_2$	$H_2 + O^{2-} \overset{\leftarrow}{\rightarrow} H_2O + 2e^-$
8.		≥0.125		$CH_4 + O^{2-} \overset{\leftarrow}{\rightarrow} 2H_2 + CO + 2e^-$
9.		≥0.125		$CH_4 + 4O^{2-} \overset{\leftarrow}{\rightarrow} 2H_2O + CO_2 + 8e^-$

under No. 1. Because CO_2 and H_2O are electrodically inactive, the only reagent that can be reduced at the electrode is O_2. Therefore, at both the electrodes, Pt and Au, the reaction of the oxygen electrode dominates when the content of CH_4 in air is low. The concentration of O_2 at Pt decreases with increasing content of CH_4, because platinum is a good catalyst for the partial oxidation of methane. At the Pt electrode, CO and H_2 appear when $p(CH_4)/p(O_2) > 0.5$ (Table 1, sequences No. 3 and 4). In the absence of oxygen, this results in the abrupt variation of electrode potentials to negative values in respect to the standard potential of the oxygen electrode.

Au is not as good catalyst as Pt for the partial oxidation reaction of methane. Therefore, only a small part of O_2 is consumed at Au during the reaction given in Table 1 under No. 7, even at high concentrations of CH_4. Au is also much worse catalyst than Pt for the reaction between hydrogen and oxygen, which produces water. Therefore, some amounts of hydrogen can be produced by the partial oxidation of methane instead of water that is produced at Pt. Simultaneous presence of O_2 and H_2 at the Au electrode results in a formation of a mixed potential. The mixed potential can also be formed due to the direct oxidation of methane at the Au|YSZ interface [4, 25] (Table 1, No. 8 and 9). Hence, the rest potential of the Au electrode is shifted in the direction of negative potentials. This phenomenon justifies the positive voltages of the Pt|YSZ|Au cell at the low concentrations of CH_4 in air.

Generally, a stationary state of gaseous electrode is settled rapidly. Therefore, it is hard to understand why the period preceding the abrupt variation of the cell voltage is sometimes so long, especially at lower temperatures, e.g. ca. 25 h for $p(CH_4)/p(O_2) = 1$ at 750°C (Fig. 3). This phenomenon can be explained by the deposition of carbon at the Pt quasi-point electrode (Table 1, No. 5) and further electro-oxidation of this carbon with formation of CO [26–28]. The rapid decrease of the cell voltage just after switching from the CH_4+air mixture back to pure air at the end of the experiment (Fig. 10) is due to this electrode reaction. It confirms also that carbon is an electroactive substance at the surface of YSZ. The voltage drop lasted longer when the operation of the cell in the range of negative voltages was longer, i.e. the deposition of carbon was larger.

The reactions collected in Table 1 may also justify the behaviour of R_e for the Pt electrode. In air atmosphere, the only electrode process occurring is

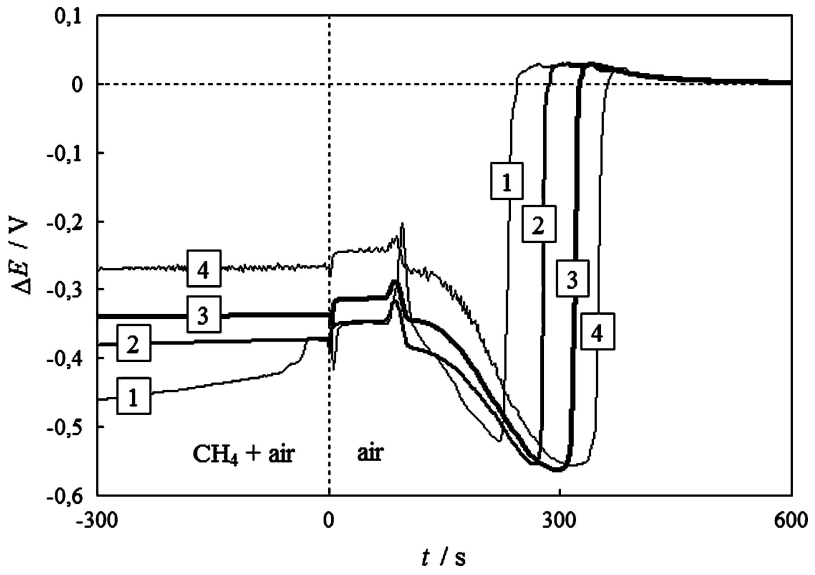

Fig. 10. Time dependences of the cell voltage after switching the atmosphere in the cell from the CH_4+air mixture [$p(CH_4)/p(O_2) = 1$] back to the pure air. $t = 0$ corresponds to the moment of switching. Durations of the cell operation since the abrupt variation of the cell voltage until switching the atmospheres: (1) 15 minutes, (2) 30 minutes, (3) 1 h and (4) 2 h. Temperature: 800°C.

the oxygen electrode reaction. Therefore, the R_e has the minimum at ΔE = ca. 0 V. After introducing the CH_4 + air mixture and just before the abrupt variation of the cell voltage, in the vicinity of the Pt electrode there is almost no O_2, H_2 and CO, which may participate in the electrode reactions. Hence, the R_e values are so high. After the abrupt variation of the cell voltage, at the electrode appear CO, H_2 and perhaps also C, which can be involved in the electrode processes. The abrupt variation of the cell voltage thus results from the variation of electrode reaction mechanism at the Pt/YSZ interface: from oxygen electrode to superposition of hydrogen, carbon monoxide and carbon electrode reactions. In the standard conditions, the potentials of the latter reactions vs. the standard oxygen electrode equal around −1 V in the range of temperatures used in this work [29, 30]. This explains why the minimum of R_e is shifted to the more negative potentials and appears at ΔE = ca. −0.5 V.

The appearance of the abrupt variation of the cell voltage at the higher ratios $p(CH_4)/p(O_2)$ at the lower temperatures can be associated with a decrease of reaction rates when the temperature is decreased.

5. Summary

The abrupt variation of the Pt|YSZ|Au cell voltage from positive to negative values was observed when the cell was fed with a mixture of CH_4+air. This variation was explained by different catalytic activities of Pt and Au for the partial oxidation of methane. Whereas the oxygen electrode reaction dominates at the Au electrode even at high concentrations of CH_4 in air, the concentration of electroactive entities in the vicinity of the Pt electrode changes with the composition of the inlet gas and approaches minimum just before the abrupt variation of the cell potential. The abrupt variation of the cell potential results from appearance of H_2 and CO at the Pt/YSZ interface. Also carbon, deposited at the Pt electrode during the experiment, participates in the overall cell reaction.

Acknowledgment

The experimental part of this work was performed at Institute of Physical Chemistry of PAS. This work was sponsored by State Committee for Scientific Research within Research Project No. 7TO8D 01621.

References

1. P. Moseley and D. Williams, *Nature*, **463**, 23 (1990).
2. K. Asuno, T. Hibino, and H. Iwahara, *J. Electrochem. Soc*., **142**, 3241 (1995).
3. T. Hibino, Y. Kuwahara, and S. Wang, *J. Electrochem. Soc.*, **146**, 2821 (1999).
4. T. Hibino, S. Wang, S. Kakimoto, and M. Sano, *Solid State Ionics*, **127**, 89 (2000).
5. T. Hibino, A. Hashimoto, T. Inoue, J. Tokunu, S.-I. Yosida, and M. Sano*, J. Electrochem. Soc.*, **147**, 2888 (2000).
6. T. Jacobsen and L. Bay, *Electrochim. Acta*, **47**, 2177 (2002).
7. L. Bay and T. Jacobsen, *Solid State Ionics*, **93**, 201 (1997).
8. T. Jacobsen, B. Zachar-Christansen, L. Bay, and M. Juhl Jorgensen, *Electrochim. Acta*, **46**, 1019 (2001).
9. N. Bonanos, B.C.H. Steele, and P. Butler, in *Impedance Spectroscopy, Emphasizing Solid Materials and Systems*, edited by J. R. Macdonald (John Willey & Sons, New York, 1987), p. 191.
10. N. Matsui and M. Takigawa, *Solid State Ionics*, **40/41**, 926 (1990).
11. T. Horita, N. Sakai, H. Yokokawa, M. Dokiya, and T. Kawada, *Solid State Ionics*, **86–88**, 1259 (1996).
12. B.A. Boukamp, *Solid State Ionics*, **143**, 47 (2001).
13. S. Onuma, A. Kaimai, K. Kawamura, Y. Nigara, T. Kawada, H. Inaba, and H. Tagawa, *J. Electrochem. Soc.,* **145**, 920 (1998).
14. G. O. Lauvstad, R. Tunold, and S. Sunde, *J. Electrochem. Soc*., 149, **E506** (2002).
15. B.A. van Hassel, B.A. Boukamp, and A.J. Burggraaf, *Solid State Ionics*, **49**, 139 (1991).
16. J. Newmann, *J. Electrochem. Soc*., **113**, 501 (1966).
17. *Fuel Cell Handbook*, 5th edition by EG&G Services Parsons Inc., Science Application International Corporation (US Department of Energy, Morgantown, 2000), p. 8–5.
18. L.S. Wang and S.A. Barnett, *J. Electrochem. Soc. Lett*., **139**, L89 (1992).
19. T. Jacobsen, B. Zachau-Christiansen, L. Ray, and S. Skaarup, in *17th Riso Int. Symp. on Materials Science* (Roskilde, Denmark, 1996).
20. A. Lasia, in *Modern Aspects of Electrochemistry*, edited by B.E. Conway, J. Bockris, and R. White (Kluwer Academic/Plenum Publishers, New York, 1999), Vol. 32, p. 143.
21. P.M. Torniainen, X. Chu, and L.D. Schmidt, *J. Catal*., **146**, 1 (1994).
22. M.A. Kahlich, A. Gasteriger, and R. Behm, *J. Catal*., **171**, 93 (1997).
23. G. Bethe and H. Kung, *Appl. Catal. A*, **194**, 43 (2000).
24. J.R. Rostrup-Nielsen and K. Aasberg-Petersen, in *Handbook of Fuel Cells-Fundamental, Technology and* Applications, edited by W. Vielstich, H.A. Gasteiger, and A. Lamm (John Wiley and Sons, Ltd., 2003, ISBN: 0-471-49936-9), Vol. 3, p. 159.
25. W.J. Fleming, *J. Electrochem. Soc*., **124**, 21 (1977).

26. T.M. Gür and R.A. Huggins, *J. Electrochem. Soc.*, **29**, 766 (1990).
27. T. Horita, N. Sakai, T. Kawada, H. Yokokawa, and M. Dokiya, *J. Electrochem. Soc.*, **142**, 2621 (1995).
28. S. Onuma, A. Kaimai, K.-I. Kawamura, Y. Nigara, T. Kawada, J. Mizusaki, H. Inaba, and H. Tagawa, *J. Electrochem. Soc.*, **145**, 920 (1998).
29. K. Sasaki and Y. Teraoka, *J. Electrochem. Soc*., **150**, A885 (2003).
30. J.R. Selman and H.C. Maru, in *Advances in Molten Salt Chemistry*, edited by G. Mamantov and J. Bronstein (Plenum Press, New York, 1981), Vol. 4, p. 176.